

# Coupling in situ and remote sensing data to assess $\alpha$ - and $\beta$ -diversity over biogeographic gradients

Maxime Lenormand,<sup>1,\*</sup> Jean-Baptiste Féret,<sup>1</sup> Guillaume Papuga,<sup>2</sup> Samuel Alleaume,<sup>1</sup> and Sandra Luque<sup>1</sup>

<sup>1</sup>*TETIS, Univ Montpellier, AgroParisTech, Cirad, CNRS, INRAE, Montpellier, France*

<sup>2</sup>*UMR 5175 CEFE, CNRS, 1919 route de Mende, 34293 Montpellier cedex 5, France*

The challenges presented by climate change are escalating and pose significant threats to global biodiversity, which in turn increases the risk of species extinctions. Therefore, meticulous monitoring efforts are necessary to mitigate the consequential impacts on both human well-being and environmental equilibrium. Biodiversity mapping is pivotal for establishing conservation priorities, often accomplished by assessing alpha, beta, and gamma diversity levels. Two main data sources, in situ and remote sensing (RS) data, are key for this task. In situ methods entail direct data collection from specific study areas, offering detailed insights into ecological patterns, albeit limited by resource constraints. Conversely, RS provides a broader observational platform, albeit at lower spatial resolution than in situ approaches. RS-derived diversity metrics have potential, particularly in linking spectral and biological diversity through high-resolution imagery for precise differentiation at fine scales. Coupling in situ and RS data underscores their complementary nature, contingent upon various factors including study scale and logistical considerations. In situ methods excel in precision, while RS offers efficiency and broader coverage. Despite prior investigations predominantly relying on limited datasets, our study endeavors to employ both in situ and RS data to assess plant and spectral species diversity across France at a high spatial resolution, integrating diverse metrics to unravel different biogeographical structures while gaining in understanding the relationship between plant and spectral diversity within and across bioregions.

## INTRODUCTION

Ecosystems are dynamic complexes of plant, animal and micro-organism communities and their abiotic environment that interact as a functional unit. Given the unprecedented nature of climate change, biological diversity is facing serious threats on a global scale [1]. Indeed, at least 25% of species are threatened with extinction, and most indicators of the state of nature suggest that they are also declining rapidly [2, 3]. These declines can have dramatic and far-reaching negative impacts on people’s well-being and the environment’s security [4]. Therefore, Ensuring accurate biodiversity monitoring at appropriate spatio-temporal resolution is important [5]. Indeed, accurate biodiversity mapping is crucial for identifying areas of high conservation priority. However, measuring species diversity is a complex task usually decomposed into three levels of diversity:  $\alpha$ -diversity,  $\beta$ -diversity and  $\gamma$ -diversity [6, 7].  $\alpha$ -diversity (species richness) and  $\beta$ -diversity (turnover in species composition) are two key components of biodiversity assessments, and the methods used to gather data, whether in situ or remote sensing approaches, can significantly impact the results.

Field data have been widely used to measure  $\alpha$ -diversity and  $\beta$ -diversity, employing various methods in different ecosystems and geographic regions. In situ data are especially valuable for studying small-scale ecological patterns and processes and capturing fine-scale differences in species composition within a particular habitat. However, estimating biodiversity with in situ data can pose various challenges. The

main limitation is the potential difficulty in obtaining comprehensive data for larger landscapes due to time and resource constraints [3, 8–11]. Nowadays, airborne and spaceborne remote sensing (RS) allow for rapid and broad-scale observation of the Earth’s surface, and dedicated methods provide a means to assess diversity metrics from RS information [8, 12], although they may not provide the same level of detail as in situ methods. The production of remotely sensed diversity metrics may be obtained from various methods [5], to be selected depending on the type of diversity metric and ecosystem. Among these methods, those relating spectral diversity to biological diversity have experienced numerous developments, as they theoretically allow assessing ecologically relevant metrics with little to no supervision in the process. This is the case for methods based on the Spectral Variation Hypothesis (SVH), which assumes that remotely sensed spatial heterogeneity reflects the heterogeneity of Earth’s surface in terms of ecological entities [13]. Depending on the system under study and the type of RS data used to observe these entities may correspond to species, habitats, or biomes. High spatial resolution imagery, with a resolution of less than 1 meter, enables the differentiation or delineation of fine-scale ecological entities, such as individual trees in a forest ecosystem. On the other hand, moderate spatial resolution imagery, ranging from 100 meters to 1 kilometre, provides an integrated view of Earth’s surface composition and processes, such as the dominant community, ecosystem or biome within the pixel or related phenology.

In situ, and RS information show strong complementarity. The relative importance between in situ and RS may be driven by multiple factors, including the scale of the study [14] and the logistic cost of acquisition of in situ or RS data. In situ methods are

---

\* Corresponding authors: maxime.lenormand@inrae.fr

well suited to fine-scale analysis, while RS is advantageous for spatial exhaustivity, upscaling of local observation and frequent revisit [12, 15]. In situ methods generally provide greater accurate ecological information, such as species identification, but they can be resource-intensive and time-consuming. RS offers efficiency and coverage but may lack the precision of ground-based observations. The relationship between diversity metrics measured with in situ and remote sensing data has been widely investigated [14–16]. So far, most empirical studies examining the relationship between  $\alpha$ -diversity and  $\beta$ -diversity assessed with in situ and remote sensing data have been based on limited datasets [11, 17]. A recent analysis conducted in the Czech Republic has shown a significant relationship between in situ and remote sensing data in assessing biodiversity [18].

In this study, we used in situ and remote sensing data to measure the diversity of plant and spectral species at high spatial resolution (> 23,000 grid cells at 5 km spatial resolution). Specifically, we relied on four diversity metrics (species richness, Shannon diversity, Simpson dissimilarity and the turnover component of the Bray-Curtis dissimilarity) to assess  $\alpha$ -diversity and  $\beta$ -diversity at different scales. Plant species were extracted from the French National Botanical Conservatory database, and spectral species were identified using a Normalised Difference Vegetation Index (NDVI) time series acquired from the MODIS satellite. First, we investigated the consistency in diversity metrics obtained from plant species inventories and RS data analysis at a national scale over the metropolitan French territory. Then, we applied a bioregionalisation network analysis [19, 20] to unravel the biogeographical structure of plant biodiversity in France, integrating both approaches. Finally, we examined the relationship between plant and spectral species diversity within and between bioregions.

## MATERIALS AND METHODS

### Datasets and Study Area

One of the main goals of the analysis proposed in this paper is to assess the level of similarity derived from two different sources of information to identify biogeographic gradients at a regional/national scale. This analysis was carried out on the metropolitan French territory, including Corsica, which covers an area of 552,000 km<sup>2</sup> (Figure 1). The map of France was divided into  $N = 23,060$  square cells of 5 km spatial resolution to define a spatial scale of analysis common for both in situ and RS data.

Information on plant species was extracted from the SIFlore database<sup>1</sup>, which was compiled by the Federation of the National Botanical Conservatories in 2016

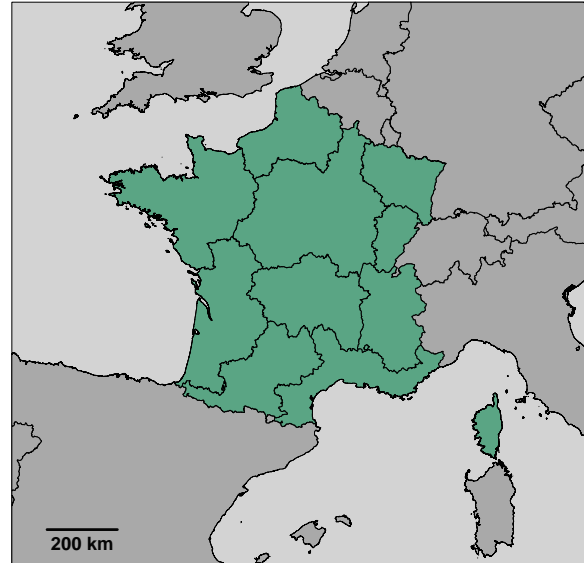


**Figure 1. Map of the France metropolitan area.** The map shows the National Botanical Conservatories' boundaries.

[21]. It integrates in situ data from the French National Botanical Conservatories, the national reference institute for flora monitoring. It contains information on the presence and abundance of  $P = 6,650$  plant species. Figure S1 in the Appendix provides the number of observations and plant species per grid cell.

RS data used for this study were based on the Terra Moderate Resolution Imaging Spectroradiometer (MODIS) Vegetation Indices (MOD13A1 Version 6)<sup>2</sup> at 500 meter spatial resolution. The data were obtained from the United States Geological Survey (USGS) data catalogue and downloaded using the R package *MODISsp*. This study focused on the Normalised Difference Vegetation Index (NDVI) time series acquired in 2010. Once downloaded, each image product was checked visually and based on pixel product quality. Images showing artefacts or poor quality were discarded. The analysis used 15 NDVI products acquired between February 18th 2010 and October 16th 2010. The method implemented in the R package *biodivMapR* was applied to the NDVI products to produce spectral species maps. This method was initially developed using high spatial resolution airborne imaging spectroscopy to assess taxonomic diversity over tropical rainforest ecosystems. The main principle of the method, applicable to any raster data, is to apply a k-means clustering analysis over an image after appropriate preprocessing and to consider each cluster as an ecological entity defined as a spectral species. The principle of the method is detailed in [22] and [23], and we will only describe the main steps here. First, we performed dimensionality reduc-

<sup>1</sup> <https://siflore.fcbn.fr>

<sup>2</sup> <https://modis.gsfc.nasa.gov/data/dataproduct/mod13.php>

tion of the NDVI time series after applying a principal component analysis. The component selection was performed based on visual interpretation of the resulting components to exclude residual artefacts and noise. A k-means clustering was then applied to the selected set of components. These clusters, defined as spectral species in the original publication from [22], do not allow species discrimination given the moderate spatial resolution of imagery data. In this study, we defined 250 spectral species to account for the diversity of seasonal patterns observed on land surface over the French territory, with a fraction of these patterns probably mainly driven by anthropic activities. At the end of the process, we obtained information on the distribution of spectral species in each 25 km<sup>2</sup> grid cell, including “presence” and “abundance” (see Figure S1 in Appendix for more details).

### Measuring $\alpha$ -diversity and $\beta$ -diversity

This study focuses on two well-known  $\alpha$ -diversity metrics: species richness, which is the number of different plant and spectral species in each cell (noted as  $R^P$  and  $R^S$ , respectively), and the normalised Shannon diversity index [24], which is computed as follows for a given cell:

$$H^P = -\frac{1}{\ln(P)} \sum_{p=1}^P F_p \ln(F_p) \quad (1)$$

Where  $F_p$  is the fraction of observations associated with the plant species  $p$  among all the plant species observations in the considered cell. The same formula can be used to compute the Shannon diversity index  $H^S$  for the spectral species by replacing  $s$  with  $p$  and  $S$  with  $P$  in Equation 1.

We relied on two  $\beta$ -diversity indices. The first index is the Simpson dissimilarity index [25], the turnover component of the Sørensen index [26], calculated between a given pair of distinct cells with the following formula:

$$\beta_{SIM}^P = \frac{\min(b_P, c_P)}{a_P + \min(b_P, c_P)} \quad (2)$$

Where  $a_P$  is the number of plant species in common between the two considered cells,  $b_P$  the number of plant species that are present in the first cell but not in the second and  $c_P$  the number of plant species that are present in the second cell but not in the first.

The second  $\beta$ -diversity considered in this study is based on the turnover component of the Bray-Curtis dissimilarity index [27], calculated between a given pair of distinct cells with the following formula:

$$\beta_{BC-bal}^P = \frac{\min(B_P, C_P)}{A_P + \min(B_P, C_P)} \quad (3)$$

Following the same reasoning,  $A_p$  may be seen as the intersection based on the species abundance in two distinct cells  $k$  and  $l$ , and  $B_p$  and  $C_p$  as the relative

complements of each cell [27], which can be formulated as:

$$A_P = \sum_{p=1}^P \min(X_{pk}, X_{pl}) \quad (4)$$

$$B_P = \sum_{p=1}^P X_{pk} - A_P \quad (5)$$

$$C_P = \sum_{p=1}^P X_{pl} - A_P \quad (6)$$

where  $X_{pk}$  stands for the number of observations of species  $p$  in cell  $k$ .

Here again, both indices were also computed for the spectral species,  $\beta_{SIM}^S$  and  $\beta_{BC-bal}^S$ , by replacing  $s$  with  $p$  and  $S$  with  $P$  in Equation 2 and 3, respectively.

### Identification of bioregions

To understand the importance of spatial context in comparing the two data sources, we needed to compare the metrics described above on a national and regional scale. To do this, we identified meaningful biogeographical regions that capture a common spatial structure between plant and spectral species.

To quantify the intensity of spatial interactions between plant and spectral species, we constructed a bipartite network, where a plant species and a spectral species are connected if they are both present in at least one cell. The edge weight represents the weighted spatial overlap between the spatial distributions of a plant species and a spectral species. The weighted overlap coefficient used in this study is based on the turnover component of the Bray-Curtis similarity index [27]. In order to remove non-significant and null values, only weighted overlap coefficients above a threshold of 0.2 were considered. More details on the construction of the bipartite network and the identification of thresholds can be found in the Appendix.

We then applied the Louvain algorithm to the bipartite network to identify network communities of plant-spectral species that share similar spatial features. Each network community contains both plant and spectral species. A network community can also be assigned to each cell by calculating the proportion of species belonging to a given community present in that cell. Since the number of plant species is significantly higher than the number of spectral species, and since these numbers can be very different from one network community to another, we decided to assign each species a weight that varies according to the type of species (plant or spectral) and its network community. Therefore, the weight of a plant (or spectral) species belonging to a given community is inversely proportional to the number of plant (or spectral) species in that community. Thus, the proportion of species present in a given cell and belonging to a given network community is equal to the ratio of the sum of the weights of these species to the total sum of the weights of the species present in that cell.

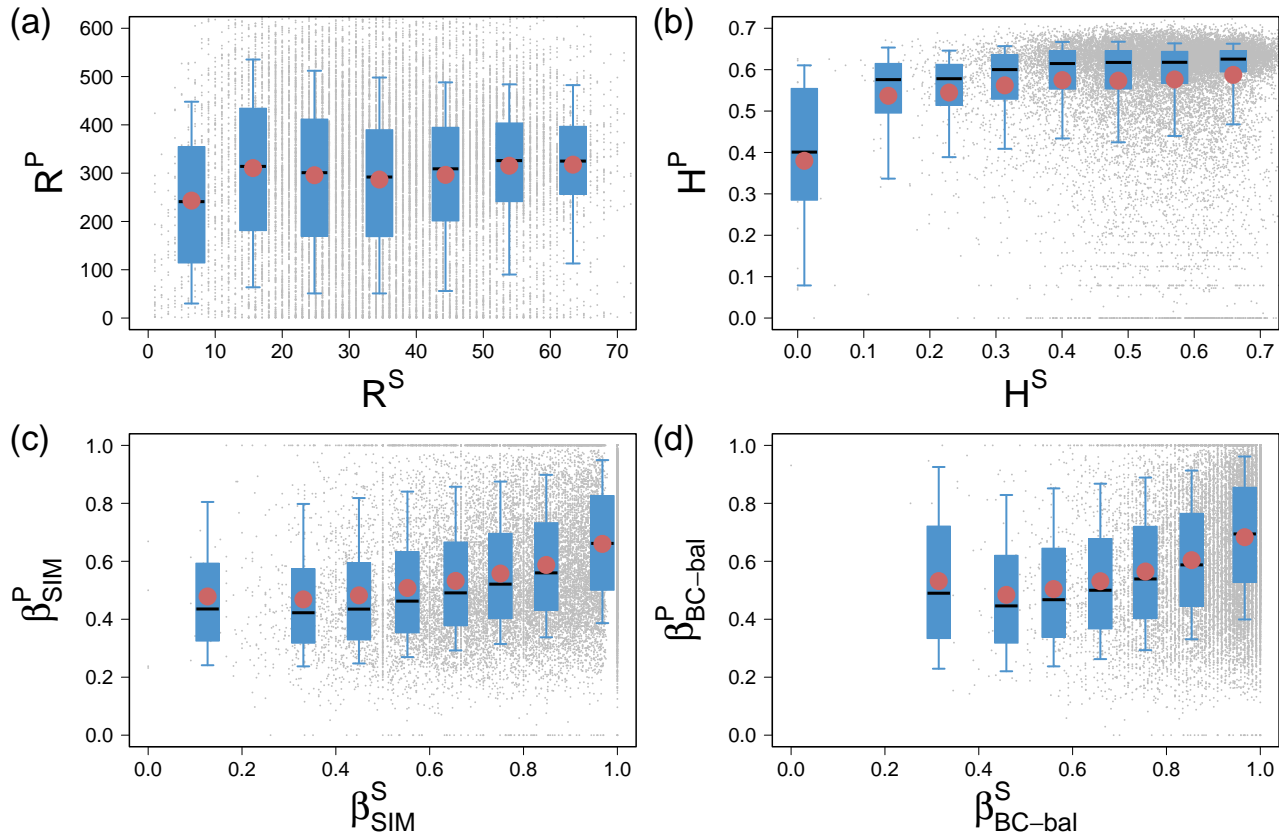


**Figure 2. Comparison of  $\alpha$ -diversity and  $\beta$ -diversity indices obtained with plant and spectral species distributions.** Comparison of the number of species per cell (a), the Shannon diversity index per cell (b), the Simpson dissimilarity index per pair of cells (c) and the turnover component of the Bray-Curtis dissimilarity index per pair of cells (d). Grey points are the scatter plot for each cell ((a) and (b)) or a sample of 20,000 pair of cells ((c) and (d)). The boxplots (D1, Q1, Q2, Q3 and D9) represent the distribution of the y-axis index in different bins of the x-axis index. The red dots represent the average in each bin. Only cells with at least one plant and spectral species were considered.

We then assigned each cell to the network community with the higher proportion of species in that cell. The set of cells belonging to a given network community is hereafter referred to as a “bioregion”. More details on the identification of bioregions can be found in the Appendix.

### Correlation measures

We focused on Pearson’s correlation coefficient to compare the four diversity metrics obtained with the plant and spectral species distributions. Unless otherwise stated, the correlation measures are based on the grid cells with at least one plant and spectral species (see *Data filtering* section in the Appendix for more details).

Correlations were measured at the national scale but also within each bioregion. Correlations were also measured between bioregions by calculating the turnover component of  $\beta$ -diversity between cells of two different bioregions.

## RESULTS

### Global analysis

Figure 2 compares the  $\alpha$ -diversity and  $\beta$ -diversity indices obtained with plant and spectral species. Figure 2a shows a scatterplot of  $R^S$  and  $R^P$  for each pair of cells. The plot shows a weak positive relationship (Pearson’s correlation coefficient of 0.037), highlighting little to no biological relationship between plot species richness and spectral richness captured. Results are globally similar when assessing  $\alpha$ -diversity using the Shannon diversity index, despite a slightly higher correlation (Pearson’s correlation of 0.072).

The correlations between the  $\beta$ -diversity indices displayed in Figure 2c and 2d show more robust trends, with a Pearson’s correlation of 0.281 for the Simpson dissimilarity index and 0.261 for the turnover component of the Bray-Curtis dissimilarity index. This depicts a general coherence in the ability of the two approaches to detect turnover between cells.

In order to understand the influence of various forms of sampling and measurement uncertainty on the results, we also computed the correlation coefficients by discarding cells with a low number of plant

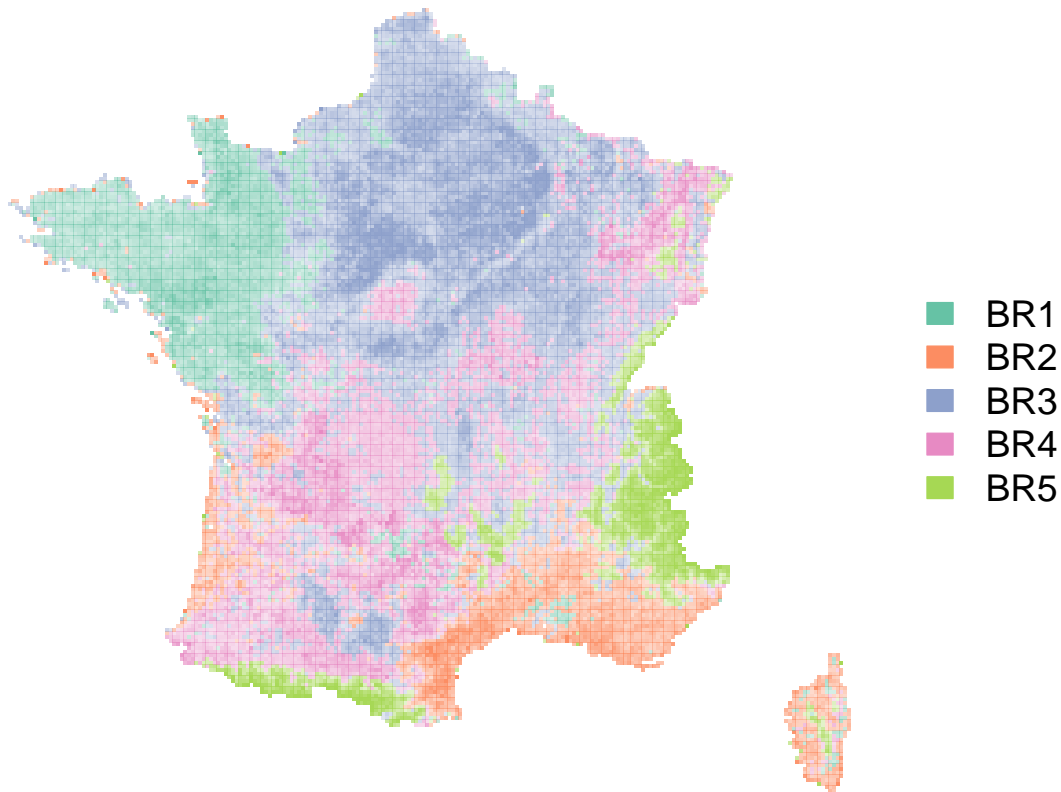


**Figure 3. Bioregion identification.** Map of France displaying the five bioregions with the colors varying from white to the baseline color of the network community assigned to each cell. The intensity of color depends on the fraction of species associated with the network community assigned to the cell.

**Table 1. Pearson’s correlation coefficient between diversity indices (and the associated 95% confidence interval) obtained with plant and spectral species distributions.**

The first column shows the results considering each cell with at least one plant and spectral species have been considered. The second column corresponds to the correlation coefficient obtained on the subsample of grid cells, filtering out cells with a low number of plant and/or spectral species, or exhibiting a relationship between the number of observations and the number of plant species deviating from the main data trend (more details are available in the *Data filtering* section in the Appendix).

Index	Pearson (no filter)	Pearson (filter)
$R$	0.037 [0.024,0.05]	0.012 [-0.003,0.027]
$H$	0.072 [0.059,0.086]	0.128 [0.113,0.143]
$\beta_{SIM}$	0.281 [0.281,0.282]	0.362 [0.362,0.362]
$\beta_{BC-bal}$	0.261 [0.261,0.261]	0.336 [0.336,0.336]

and/or spectral species or exhibiting a relationship between the number of observations and the number of plant species deviating from the main data trend (more details available in *Data filtering* section in Appendix). The results obtained with this new sample of 16,551 cells are available in Table 1. These results confirm the very weak correlation between  $R^S$  and  $R^P$ . However, we observe an increase of Pearson’s correlation between  $H^S$  and  $H^P$  (from 0.072 to 0.128),

$\beta_{SIM}^S$  and  $\beta_{SIM}^P$  (from 0.281 to 0.362), and,  $\beta_{BC-bal}^S$  and  $\beta_{BC-bal}^P$  (from 0.261 to 0.336).

### Bioregional analysis

We applied the Louvain algorithm [28] and identified five plant-spectral communities in the bipartite network. The intensity of the spatial interaction (i.e. the weight of the bipartite network) between plant and spectral species according to the network community is available in the *Identification of bioregions* section in the Appendix. The percentages of plant species, spectral species and grid cells by network community are available in Table S1 in Appendix.

By assigning a network community to each grid cell, we identified five bioregions reflecting the biogeographical structure of France based on plant and spectral species distributions (Figure 3). The biogeographical structure shown is consistent with several empirical studies, such as that of GRECO<sup>3</sup> on the forests of France [29]. The first bioregion (BR1) covers much of the westernmost part of France and adja-

<sup>3</sup> <https://inventaire-forestier.ign.fr/spip.php?article773>

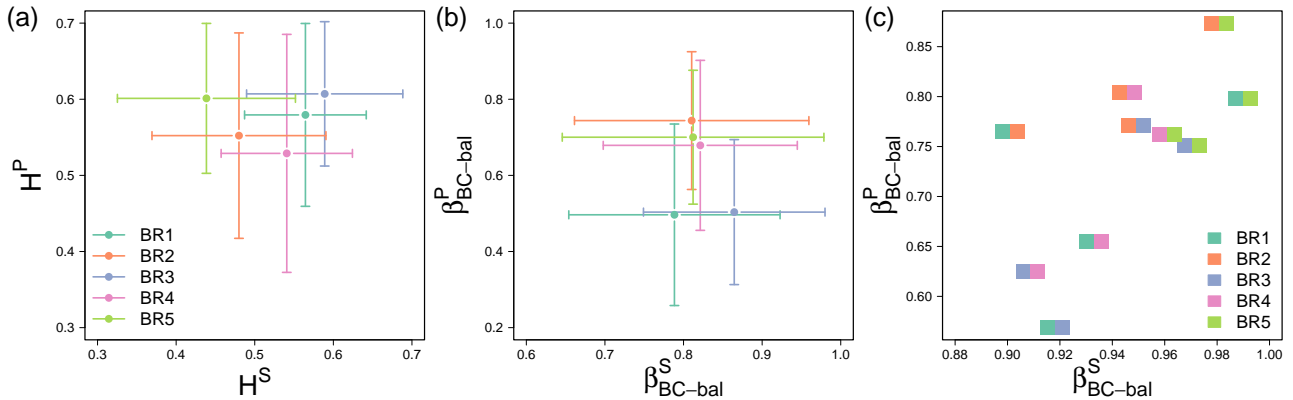


**Figure 4. Comparison of  $\alpha$ -diversity and  $\beta$ -diversity indices obtained with plant and spectral species distributions within and between bioregions.** (a) Average Shannon diversity index per cell within bioregion (and its associated standard deviations). (b) Average turnover component of the Bray-Curtis dissimilarity index per pair of cells within bioregion (and its associated standard deviations). (c) Average turnover component of the Bray-Curtis dissimilarity index per pair of cells between bioregions. Standard deviations are available in Table S2 in the Appendix.

cent regions. This zone is characterised by a marked oceanic climate and a substratum dominated by the Hercynian crystalline rocks of the Armorican massif. The second bioregion (BR2) corresponds mainly to France’s Mediterranean zone and includes the rocky west’s coastal vegetation. The third bioregion (BR3) mainly covers the plains of northern France. Under the oceanic influence, these areas include large agricultural plains mainly occupied by neutral-basic soils and Quaternary sedimentary deposits. The fourth bioregion (BR4) is a relatively heterogeneous group distributed throughout the country. It includes large areas of medium-sized mountains (in the Massif Central and the Vosges) and various lowland areas. The fifth bioregion (BR5) covers high mountain areas, mainly in the Alps, the Jura, and the southern Pyrenees, with more peripheral zones in Corsica, the Massif Central, and the Vosges mountain ranges. The substratum is largely heterogeneous, but the bioregion is characterised by a common topography and vegetation structure from the mountain to the alpine zone.

We plot in Figure 4 the average values of two  $\alpha$ -diversity and  $\beta$ -diversity ( $H$  and  $\beta_{BC-bal}$ ) obtained within each bioregion and also between bioregions for the  $\beta$ -diversity. Figure 4a shows the relationship between spectral and species  $\alpha$ -diversity by bioregion. Globally, the  $H$  index behaves similarly for plant and spectral species within the same bioregion. Only BR5 (mountain region), rich in plant species, deviates from the overall pattern, with plant  $\alpha$ -diversity higher than spectral  $\alpha$ -diversity.

Figure 4b shows the relationship between the Bray-Curtis turnover estimated from flora and spectral data within each bioregion. The  $\beta$ -diversity index obtained with spectral species is spread over a smaller range of values (0.78 to 0.86) than that obtained with plant species (0.5 to 0.78). The plant data divide the bioregions into two groups: BR2/BR5/BR4 with high values for the plant index, reflecting greater spatial heterogeneity of plant communities, and BR1/BR3 with

lower values. Bioregion BR3 has the highest value for the spectral species but one of the lowest for the plant species. This can be partially explained by the prevalence of natural and semi-natural habitats in the first group (Mediterranean, middle and high mountains) in preference to an agricultural matrix, suggesting a certain biotic homogenisation despite the marked landscape structure.

Figure 4c represents the average Bray-Curtis turnover between each pair of bioregions estimated with plant and spectral species. The two approaches have a positive relationship, with the highest values for the Mediterranean (BR2) and mountain (BR5) zones, which are very different from the other regions for both approaches. Only the BR1-BR2 comparison shows a higher dissimilarity for plant species than for spectral species, probably indicating a very different species pool (medio-European vs. Mediterranean) but a less dissimilar vegetation structure. Conversely, the lowest values between BR1, BR3 and BR4 reflect the greater similarity between these entities, with the two lowland bioregions with an agricultural matrix (BR1/BR3) showing the greatest similarity.

Figure 5 shows Pearson’s correlation coefficients (and their 95% confidence intervals) by bioregion. Figure 5a shows the correlation coefficient between Shannon diversity indices obtained with plant and spectral species in the whole study area (i.e. “All”) and within bioregions. The overall correlation is globally weak, with values per bioregion ranging from -0.1 to 0.17. BR4 shows a weaker correlation and BR5 a stronger one, reflecting a more robust relationship between  $\alpha$ -diversity estimated with plant and spectral species. Thus, bioregions have no substantial structuring effect on the correlation between  $\alpha$ -diversity estimated with plant and spectral species.

Figure 5b displays the Pearson correlation coefficient between plant and spectral species obtained with the turnover component of the Bray-Curtis dissimilarity index for the whole study area (i.e. “All”)

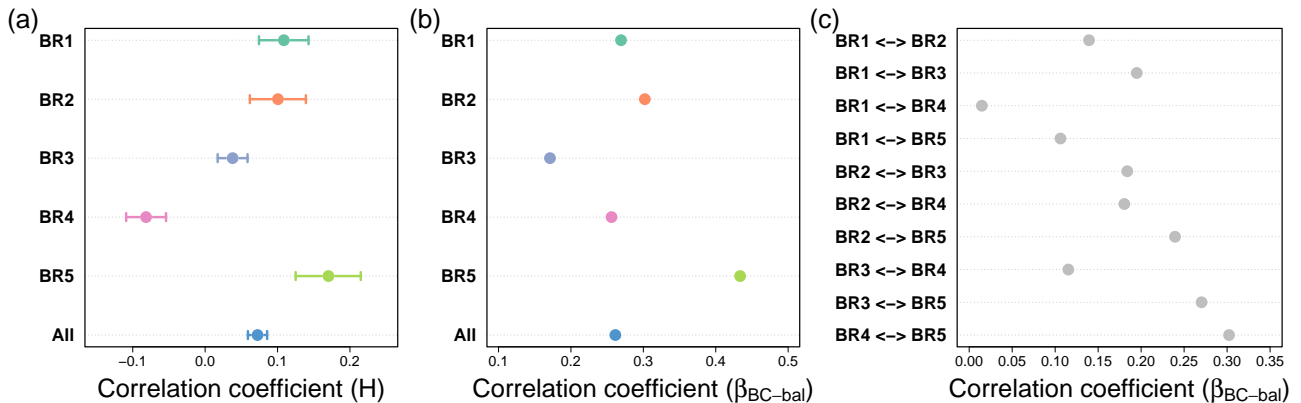


**Figure 5. Correlation between  $\alpha$ -diversity and  $\beta$ -diversity indices obtained with plant and spectral species distributions within and between bioregions.** (a) Pearson’s correlation coefficients between Shannon diversity indices obtained with plant and spectral species for each bioregion and for the whole study area. (b) Pearson’s correlation coefficients between the turnover component of the Bray-Curtis dissimilarity index obtained with plant and spectral species for each bioregion and for the whole study area. (c) Pearson’s correlation coefficients between the turnover component of the Bray-Curtis dissimilarity index obtained with plant and spectral species between bioregions. Error bars indicating the 95% confidence interval are too small to be seen for the turnover component of the Bray-Curtis dissimilarity index.

and within bioregions (Figure 5b). We observed correlation coefficients close to the average for the BR1/BR2/BR4 bioregions (0.3) and slightly lower for BR3 (0.17). Only BR4 (mountainous zone) exhibits a stronger correlation, highlighting a higher plant turnover when spectral turnover is detected.

Finally, Figure 5c displays the Pearson correlation coefficient between plant and spectral species obtained with the turnover component of the Bray-Curtis dissimilarity index between each bioregion (Figure 5c). These coefficients are mostly centred around the value of 0.15, with extremes ranging from 0.01 (BR1/BR5) to 0.3 (BR4/BR5). These high values suggest that a high turnover of spectral species translates into a high turnover of plant species.

## DISCUSSION

Analysing the spatial structure of diversity patterns is key to understanding and managing biodiversity [5, 30–33]. These approaches can benefit from new technologies, particularly high-resolution spatial imagery. In this study, we compared and combined field data describing plant communities in mainland France with remote sensing data based on the Spectral Variation Hypothesis to describe the structure of the French biogeographical structure using a network approach. We analysed the consistency of the two sources of information to estimate  $\alpha$ -diversity and  $\beta$ -diversity within and between bioregions. We found a coherent biogeographic structure despite a heterogeneous floristic dataset. Through this discussion, we will address how spectral approaches can prove complementary to in situ data to assess different facets of the biogeographic diversity of plant assemblages. We will also discuss the limitations of the two approaches and how future methodological developments will al-

low them to be better combined.

### Comparison of $\alpha$ -diversity

The first step in our study was to analyse the consistency of the two approaches, spectral and field, for estimating  $\alpha$ -diversity within each pixel. The spectral approach is based on virtual “spectral species”, defined by a set of spectro-temporal features corresponding to a NDVI time-series. In contrast, the field approach is based on a list of species derived from the synthesis of opportunistic inventories. The two approaches showed a lack of correlation for taxonomic richness (spectral and plant) and a very weak correlation for Shannon’s diversity index. This was independent of the detected bioregions, with only the high mountains showing a slightly stronger correlation coefficient.

This lack of consistency is not surprising given the spatial heterogeneity of floristic inventories (Figure S1b in the Appendix) and the spatial patterns of spectral species richness. Indeed, the geospatial approach detects the highest levels of richness in the agricultural areas of north-central France and the lowest levels of richness in the high and medium mountain areas and the Mediterranean belt. This is in complete contrast to the empirically known patterns of plant biodiversity [34] and mainly reflects the internal structure of the spectral species index [15]. Indeed, it is probable that the local spatial heterogeneity, occurring at a scale larger than 10 meters, induced by various components within agricultural environments (such as fields, meadows, and field margins), surpasses that found in more natural environments like high mountain grasslands or Mediterranean scrub. Therefore, it is reasonable to assume that spectral species are not directly equivalent to biological species, and the estimation of

the former relies on local contingencies that are independent of plant biodiversity.

### Comparison of $\beta$ -diversity

Secondly, the analysis of  $\beta$ -diversity using taxonomic and spectral approaches showed greater consistency between the two approaches. The analysis of  $\beta$ -diversity patterns emphasized a turnover between pairs of pixels, thereby incorporating unit identity (both spectral and taxonomic) to measure shifts within communities. This approach revealed a notable level of global consistency, with results consistently observed across various bioregions, indicating the absence of significant local regional outliers in the overall findings. Nevertheless, it's worth noting that this signal exhibited slight elevation in high mountain regions and a decrease in lowland arable areas. One possible interpretation is that turnover in the mountains is structured by a marked change in natural habitats, the taxonomic composition of which is largely specific. This change in natural habitat is detected by an equivalent change in spectral species and floristic assemblages. Alternatively, the spectral species will detect different crops (particularly due to their specific phenology), which, oppositely, form a globally homogeneous habitat with poor flora (i.e. ruderal weeds and generalist species).

In addition to these methods, comparing the beta diversity of pixels from distinct bioregions provides valuable insights into the inferred degree of ecological differentiation between two spatial entities. Taxonomic and spectral approaches detect the same strong turnover between the Mediterranean (BR2), high mountain (BR5) and mid-mountain (BR4) regions. These zones differ greatly in their species assemblages, with the most marked transition between the hot, dry Mediterranean zone (BR3) and the cold high mountain zone (BR5). In the latter, the flora is under a Euroasian influence, starkly contrasting with Mediterranean biodiversity. This is also reflected in the marked contrasts between the habitats that dominate the landscape: among open habitats, Alpine perennial grassland differs in every way from open scrubland with much bare soil; similarly, deciduous and mixed coniferous/hardwood forests exhibit different spectral signals from Mediterranean evergreen forests, ultimately reflected in a marked turnover of spectral species. In contrast, the agricultural plain zones (BR3) and the oceanic zone on an acid substratum (BR1) show the greatest floristic similarity and a strong spectral similarity. This reflects a shared biogeographical influence, with widely distributed temperate plant species and relatively close spectral species, suggesting similar agricultural landscape components (e.g. fields and grasslands) and deciduous forests.

Therefore, while spectral approaches have shown limitations in assessing patterns of floristic richness, they are generally consistent in evaluating spatial dif-

ferentiation when turnover is taken into account.

### Combining remote sensing and field data to identify bioregions

The approach proposed in this article allows for identifying bioregions based on a minimum common spatial structure between plant and spectral species (Figure 3). The overall result is consistent with the bioregionalisation proposed by several authors [20, 29]. The high mountain areas of France, in particular the Alps and the Pyrenees, are well-defined. This vegetation type is also found on the summits of the lower massifs, including the Vosges, the Jura, the Massif Central and Corsica. The common floristic influences and vegetation structure between mixed coniferous and deciduous forests, alpine meadows and high rocky environments create uniformity in these areas. The presence of snow for part of the year reinforces this similarity. The delineation of the Mediterranean zone is also consistent with recent work [20]. There is a link with the Atlantic coastal areas, which, although highly contrasted in species assemblages, could contain a relatively similar structuring of coastal habitats (sandy dune or rocky coastline).

Therefore, coupling remote sensing and in situ data could significantly contribute to fill gaps in biodiversity monitoring [35]. Firstly, it is generally accepted that the quality of taxonomic field data will condition the possibility of carrying out relevant bioregionalisation [36]. In particular, the spatial accuracy and the sampling effort [37, 38] will condition the final resolution of the work and define the grain with which the spatial structure of bioregions can be assessed. Despite the constant increase in the amount of naturalist data, the latter remains disparate in many areas of the globe, and the absence of structured sampling limits the observation pressure on certain taxonomic groups [39–41]. Secondly, it is important to remember that bioregionalisation approaches are almost always carried out at a given time: collecting field data on large spatial scales is far too costly to be replicated over time to assess bioregions' temporal dynamics. This approach would enable us to dynamically understand bioregions, which could be relevant in transition zones between bioregions in the context of climate change and related migration [20].

### Limitations of the study

The definition of a bioregion depends on the quality of the dataset we are working with. Here, floristic data were aggregated at a national level based on the work of botanical conservatories assigned to different administrative regions. This dataset had significant gaps, especially in areas that did not recently have a conservatory (e.g. in the northeast) (see Figure S1b in the Appendix). At the same time, sampling pressure

within our dataset is highly variable between institutions (Figure S1a in the Appendix), suggesting a highly variable state of knowledge within each region. These biases have affected the delineation of bioregions, although mitigated by the information derived from spectral approaches. In the future, the major challenge will be understanding the relative contribution of the two approaches at different locations in the network to partition the importance of taxonomic and spectral sources on the final result.

In addition to these sampling issues, there is also the question of taxonomic resolution. The data for this paper have been aggregated at a certain level according to a common reference system to standardise the taxonomic level. The main drawback of this approach is that it flattens some of the knowledge by removing the finesse of identifying population groups, often defined at the subspecies level, which could prove informative for understanding certain biogeographical structures. In addition, taxonomic units are considered at the same level, with no interdependence to their evolutionary similarity. A potential development of these methods could be to become taxonomically explicit by incorporating a distance between taxa to refine the definition of bioregions and reveal a deeper evolutionary structure.

Finally, it should be noted that the statistically classified individuals (i.e. pixels) are independent within the analysis. A possible improvement would be to make them spatially explicit, allowing the inference of a bioregion to under-sampled pixels based on spectral species coupled with a biogeographic signal inferred from the spatial proximity of other pixels.

## Perspectives

Identifying bioregions is essential for managing ecosystems and developing conservation policies [42]. Creating coherent geographical clusters based on shared biodiversity is crucial for better understanding a region's ecological and evolutionary structure. These tools are particularly useful for projects such as ecological restoration and the establishment of protected areas [43].

Therefore, it may be worthwhile to develop these approaches in areas where taxonomic knowledge is limited and for groups of species that need better documentation. Improving the definition of bioregions, coupled with geospatial data, proves relevant and opens the way to developing an approach that integrates ecologically, spatially, and phylogenetically explicit advances.

## Data and materials availability

All data, code, and materials used in the present paper are available online (<https://gitlab.com/maximelenormand/plant-spectral-diversity>)

## ACKNOWLEDGMENTS

The authors would like to thank the Federation of the National Botanical Conservatories (CBN) and the French Biodiversity Agency (OFB) for providing species data from the SIFlore database. A special thank goes to Olivier Argagnon, from CBN Med, for useful discussions.

- 
- [1] B. J. Cardinale, J. E. Duffy, A. Gonzalez, D. U. Hooper, C. Perrings, P. Venail, A. Narwani, G. M. Mace, D. Tilman, D. A. Wardle, A. P. Kinzig, G. C. Daily, M. Loreau, J. B. Grace, A. Larigauderie, D. S. Srivastava, and S. Naeem. Biodiversity loss and its impact on humanity. *Nature*, 486(7401):59–67, 2012.
- [2] S. Díaz, J. Settele, E. S. Brondízio, H. T. Ngo, J. Agard, A. Arneth, P. Balvanera, K. A. Brauman, S. H. M. Butchart, K. M. A. Chan, L. A. Garibaldi, K. Ichii, J. Liu, S. M. Subramanian, G. F. Midgley, P. Miloslavich, Z. Molnár, D. Obura, A. Pfaff, S. Polasky, A. Purvis, J. Razzaque, B. Reyers, R. R. Chowdhury, Y.-J. Shin, I. Visseren-Hamakers, K. J. Willis, and C. N. Zayas. Pervasive human-driven decline of life on Earth points to the need for transformative change. *Science*, 366(6471):eaax3100, 2019.
- [3] D. Tickner, J. J. Opperman, R. Abell, M. Acreman, A. H. Arthington, S. E. Bunn, S. J. Cooke, J. Dalton, W. Darwall, G. Edwards, I. Harrison, K. Hughes, T. Jones, D. Leclère, A. J. Lynch, P. Leonard, M. E. McClain, D. Muruvu, J. D. Olden, S. J. Ormerod, J. Robinson, R. E. Tharme, M. Thieme, K. Tockner, M. Wright, and L. Young. Bending the Curve of Global Freshwater Biodiversity Loss: An Emergency Recovery Plan. *BioScience*, 70(4):330–342, 2020.
- [4] T. Newbold, G. L. Adams, G. Albaladejo Robles, E. H. Boakes, G. Braga Ferreira, A. S. A. Chapman, A. Etard, R. Gibb, J. Millard, C. L. Outhwaite, and J. J. Williams. Climate and land-use change homogenise terrestrial biodiversity, with consequences for ecosystem functioning and human well-being. *Emerging Topics in Life Sciences*, 3(2):207–219, 2019.
- [5] R. Wang and J. A. Gamon. Remote sensing of terrestrial plant biodiversity. *Remote Sensing of Environment*, 231:111218, 2019.
- [6] R. H. Whittaker. Vegetation of the Siskiyou Mountains, Oregon and California. *Ecological Monographs*, 30(3):279–338, 1960.
- [7] R. H. Whittaker. Evolution and Measurement of Species Diversity. *Taxon*, 21(2/3):213–251, 1972.
- [8] S. Luque, N. Pettorelli, P. Vihervaara, and M. Wegmann. Improving biodiversity monitoring using satellite remote sensing to provide solutions towards the

- 2020 conservation targets. *Methods in Ecology and Evolution*, 9(8):1784–1786, 2018.
- [9] N. Pettorelli, H. Schulte to Bühne, A. Tulloch, G. Dubois, C. Macinnis-Ng, A. M. Queirós, D. A. Keith, M. Wegmann, F. Schrodtt, M. Stellmes, R. Sonnenschein, G. N. Geller, S. Roy, B. Somers, N. Murray, L. Bland, I. Geijzendorffer, J. T. Kerr, S. Broszeit, P. J. Leitão, C. Duncan, G. El Serafy, Kate S. He, J. L. Blanchard, R. Lucas, P. Mairota, T. J. Webb, and E. Nicholson. Satellite remote sensing of ecosystem functions: opportunities, challenges and way forward. *Remote Sensing in Ecology and Conservation*, 4(2):71–93, 2018.
- [10] D. Rocchini, N. Salvatori, C. Beierkuhnlein, A. Chiarucci, F. de Boissieu, M. Förster, C. X. Garzon-Lopez, T. W. Gillespie, H. C. Hauffe, K. S. He, B. Kleinschmit, J. Lenoir, M. Malavasi, V. Moudrý, H. Nagendra, D. Payne, P. Šímová, M. Torresani, M. Wegmann, and J.-B. Féret. From local spectral species to global spectral communities: A benchmark for ecosystem diversity estimate by remote sensing. *Ecological Informatics*, 61:101195, March 2021.
- [11] E. Chraïbi, H. Arnold, S. Luque, A. Deacon, A. E. Magurran, and J.-B. Féret. A Remote Sensing Approach to Understanding Patterns of Secondary Succession in Tropical Forest. *Remote Sensing*, 13(11):2148, 2021.
- [12] S. L. Ustin and E. M. Middleton. Current and near-term advances in Earth observation for ecological applications. *Ecological Processes*, 10(1):1, 2021.
- [13] G. P. Asner, R. E. Martin, D. E. Knapp, R. Tupayachi, C. B. Anderson, F. Sinca, N. R. Vaughn, and W. Llactayo. Airborne laser-guided imaging spectroscopy to map forest trait diversity and guide conservation. *Science*, 355(6323):385–389, 2017.
- [14] D. Rocchini, D. McGlenn, C. Ricotta, M. Neteler, and T. Wohlgemuth. Landscape complexity and spatial scale influence the relationship between remotely sensed spectral diversity and survey-based plant species richness. *Journal of Vegetation Science*, 22(4):688–698, 2011.
- [15] D. Rocchini, L. Dadalt, L. Delucchi, M. Neteler, and M. W. Palmer. Disentangling the role of remotely sensed spectral heterogeneity as a proxy for North American plant species richness. *Community Ecology*, 15(1):37–43, 2014.
- [16] F. Marzioletti, S. Cascone, L. Frate, M. Di Febbraro, A. T. R. Acosta, and M. L. Carranza. Measuring Alpha and Beta Diversity by Field and Remote-Sensing Data: A Challenge for Coastal Dunes Biodiversity Monitoring. *Remote Sensing*, 13:1928, 2021.
- [17] F. E. Fassnacht, J. Müllerová, L. Conti, M. Malavasi, and S. Schmidlein. About the link between biodiversity and spectral variation. *Applied Vegetation Science*, page e12643, 2022.
- [18] M. Perrone, M. Di Febbraro, L. Conti, J. Divíšek, M. Chytrý, P. Keil, M. L. Carranza, D. Rocchini, M. Torresani, V. Moudrý, P. Šímová, D. Prajzlerová, J. Mällerová, J. Wild, and M. Malavasi. The relationship between spectral and plant diversity: Disentangling the influence of metrics and habitat types at the landscape scale. *Remote Sensing of Environment*, 293:113591, 2023.
- [19] A. Antonelli. Biogeography: Drivers of bioregionalization. *Nature Ecology & Evolution*, 1(4):0114, 2017.
- [20] M. Lenormand, G. Papuga, O. Argagnon, M. Soubeyrand, G. De Barros, S. Alleaume, and S. Luque. Biogeographical network analysis of plant species distribution in the Mediterranean region. *Ecology and Evolution*, 9(1):237–250, 2019.
- [21] A. Just, J. Gouvil, J. Millet, V. Bouillet, T. Milon, I. Mandon, and B. Dutrève. Siflore, a dataset of geographical distribution of vascular plants covering five centuries of knowledge in france: Results of a collaborative project coordinated by the federation of the national botanical conservatories. *Phytokeys*, (56):47–60, 2016.
- [22] J.-B. Féret and G. P. Asner. Mapping tropical forest canopy diversity using high-fidelity imaging spectroscopy. *Ecological Applications*, 24(6):1289–1296, 2014.
- [23] J.-B. Féret and F. de Boissieu. biodivMapR: An R package for alpha- and beta-diversity mapping using remotely sensed images. *Methods in Ecology and Evolution*, 11(1):64–70, 2020.
- [24] C. E. Shannon. A mathematical theory of communication. *The Bell System Technical Journal*, 27:379–423, 1948.
- [25] G. G. Simpson. Mammals and the nature of continents. *American Journal of Science*, 241(1):1–31, 1943.
- [26] A. Baselga. Partitioning the turnover and nestedness components of beta diversity. *Global Ecology and Biogeography*, 19(1):134–143, 2010.
- [27] A. Baselga. Separating the two components of abundance-based dissimilarity: balanced changes in abundance vs. abundance gradients. *Methods in Ecology and Evolution*, 4(6):552–557, 2013.
- [28] V.D. Blondel, J.L. Guillaume, R. Lambiotte, and E.L.J.S. Mech. Fast unfolding of communities in large networks. *J. Stat. Mech*, page P10008, 2008.
- [29] J.-D. Bontemps, J.-C. Hervé, and A. Denardou. Partition idéalisée et régionalisée de la composition en espèces ligneuses des forêts françaises. *Écoscience*, 26(4):291–308, 2019.
- [30] J. S. Carvalho, B. Graham, G. Bocksberger, F. Maisels, E. A. Williamson, S. Wich, T. Sop, B. Amarasekaran, B. Barca, A. Barrie, R. A. Bergl, C. Boesch, H. Boesch, T. M. Brncic, B. Buys, R. Chancellor, E. Danquah, O. A. Doumbé, S. Y. Le-Duc, A. Galat-Luong, J. Ganas, S. Gatti, A. Ghiurghi, A. Goedmakers, N. Granier, D. Hakizimana, B. Haurez, J. Head, I. Herbinger, A. Hillers, S. Jones, J. Junker, N. Maputla, E.-N. Manasseh, M. S. McCarthy, M. Molokwu-Odozi, B. J. Morgan, Y. Nakashima, P. K. N’Goran, S. Nixon, L. Nkambi, E. Normand, L. D.Z. Nzooh, S. H. Olson, L. Payne, C.-A. Petre, A. K. Piel, L. Pintea, A. J. Plumptre, A. Rundus, A. Serckx, F. A. Stewart, J. Sunderland-Groves, N. Tagg, A. Todd, A. Vosper, J. F.C. Wenceslau, E. G. Wessling, J. Willie, and H. S. Kühl. Predicting range shifts of African apes under global change scenarios. *Diversity and Distributions*, 27(9):1663–1679, 2021.
- [31] C. Geppert, G. Perazza, R. J. Wilson, A. Bertolli, F. Prosser, G. Melchiori, and L. Marini. Consistent population declines but idiosyncratic range shifts in Alpine orchids under global change. *Nature Communications*, 11(1):5835, 2020.
- [32] C. A. Hallmann, A. Ssymank, M. Sorg, H. de Kroon, and E. Jongejans. Insect biomass decline scaled

- to species diversity: General patterns derived from a hoverfly community. *Proceedings of the National Academy of Sciences*, 118(2):e2002554117, 2021.
- [33] I. Overcast, M. Ruffley, J. Rosindell, L. Harmon, P. A. V. Borges, B. C. Emerson, R. S. Etienne, R. Gillespie, H. Krehenwinkel, D. L. Mahler, F. Massol, C. E. Parent, J. Patiño, B. Peter, B. Week, C. Wagner, M. J. Hickerson, and A. Rominger. A unified model of species abundance, genetic diversity, and functional diversity reveals the mechanisms structuring ecological communities. *Molecular Ecology Resources*, 21(8):2782–2800, 2021.
- [34] I. Biurrun et al. Benchmarking plant diversity of Palaearctic grasslands and other open habitats. *Journal of Vegetation Science*, 32(4):e13050, 2021.
- [35] P. Vihervaara, A.-P. Auvinen, L. Mononen, M. Törmä, P. Ahlroth, S. Anttila, K. Böttcher, M. Forsius, J. Heino, J. Heliölä, M. Koskelainen, M. Kuussaari, K. Meissner, O. Ojala, S. Tuominen, M. Viitasalo, and R. Virkkala. How Essential Biodiversity Variables and remote sensing can help national biodiversity monitoring. *Global Ecology and Conservation*, 10:43–59, 2017.
- [36] H. Kreft and W. Jetz. A framework for delineating biogeographical regions based on species distributions. *Journal of Biogeography*, 37(11):2029–2053, 2010.
- [37] A. R. Giraud and V. Arzamendia. Descriptive bioregionalisation and conservation biogeography: what is the true bioregional representativeness of protected areas? *Australian Systematic Botany*, 30(5–6):403–413, 2018.
- [38] S. Ferrier. Mapping Spatial Pattern in Biodiversity for Regional Conservation Planning: Where to from Here? *Systematic Biology*, 51(2):331–363, 2002.
- [39] T. August, R. Fox, D. B. Roy, and M. J. O. Pocock. Data-derived metrics describing the behaviour of field-based citizen scientists provide insights for project design and modelling bias. *Scientific Reports*, 10(1):11009, 2020.
- [40] O. J. Reichman, Matthew B. Jones, and Mark P. Schildhauer. Challenges and Opportunities of Open Data in Ecology. *Science*, 331(6018):703–705, 2011.
- [41] N. J. B. Isaac, A. J. van Strien, T. A. August, M. P. de Zeeuw, and D. B. Roy. Statistics for citizen science: extracting signals of change from noisy ecological data. *Methods in Ecology and Evolution*, 5(10):1052–1060, 2014.
- [42] S. N. C. Woolley, S. D. Foster, N. J. Bax, J. C. Currie, D. C. Dunn, C. Hansen, N. Hill, T. D. O’Hara, O. Ovaskainen, R. Sayre, J. P. Vanhatalo, and P. K. Dunstan. Bioregions in Marine Environments: Combining Biological and Environmental Data for Management and Scientific Understanding. *BioScience*, 70(1):48–59, 2020.
- [43] G. F. Smith and M. M. Wolfson. Mainstreaming biodiversity: the role of taxonomy in bioregional planning activities in South Africa. *TAXON*, 53(2):467–468, 2004.

## APPENDIX

## Data description

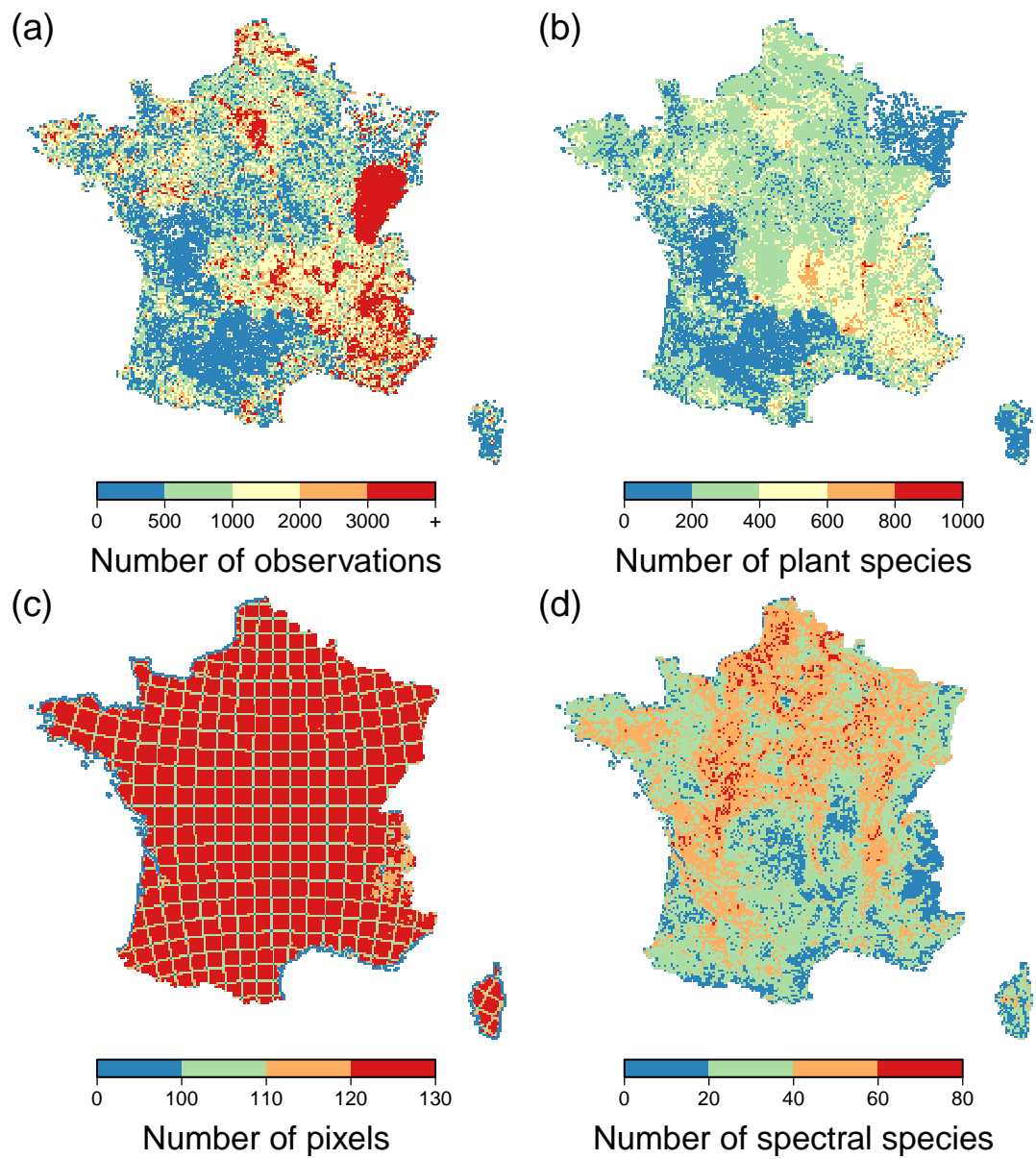


**Figure S1. Data description.** Distributions of the number of botanic observations (a), number of plant species (b), number of pixels (c) and number of spectral species (d) per  $5 \times 5 \text{ km}^2$  grid cell.

### Data filtering

In this study, the map of France has been divided into  $N = 23,060$  square cells. However, some cells have very few observations for the plant species or pixels for the spectral species. First, we only considered cells with at least one observation and one pixel representing 93% of the cells. Unless otherwise specified, the correlation measures presented in the paper are based on these grid cells.

Then, two consecutive filters have been considered. In order to filter out cells with a number of plant/spectral species lower than the number of observations/pixels we discarded all the cells with less than 200 observations or 20 pixels as can be observed in Figure S2. We obtained a sample of 18,192 cells (79% of the original sample).

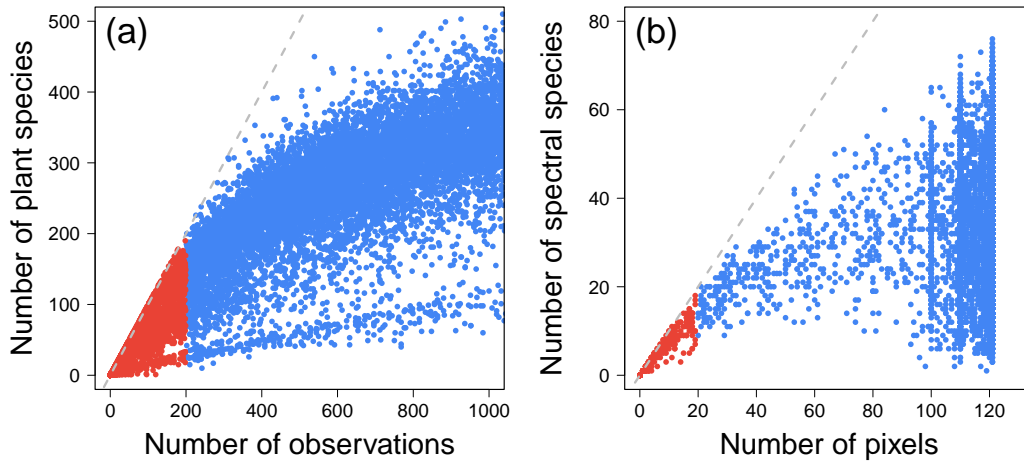


**Figure S2. Identification of the first filter thresholds.** (a) Number of plant species as a function of the number of observations. Each point represents a cell. The red points represents the cells exhibiting a number of observations lower than 200. (b) Number of spectral species as a function of the number of pixels. Each point represents a cell. The red points represents the cells exhibiting a number of pixels lower than 20.

We finally filtered out 1,610 additional cells by applying a second filter to discard cells exhibiting a relationship between the number of observations and the number of plant species deviating from the main data trend (based on Equation S1 that can be visualized in Figure S3).

$$R^P > 1.5 \cdot O^{1/1.5} \quad (1)$$

At the end of the process we obtained a sample of 16,551 cells (72% of the original sample).

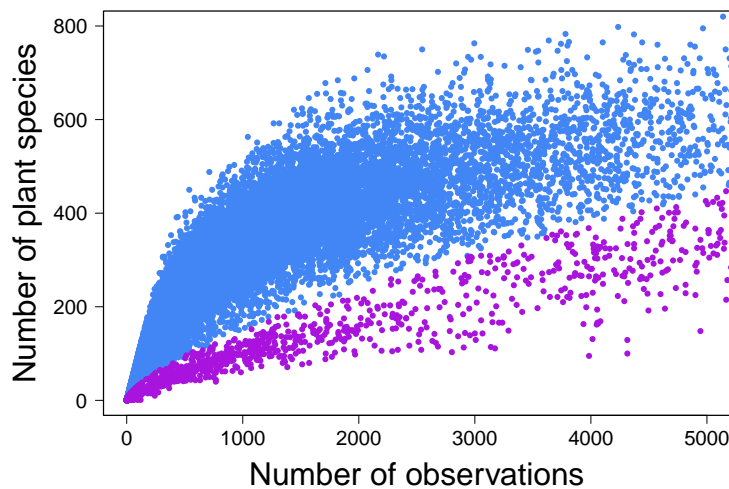


**Figure S3. Identification of the second filter relationship.** Number of plant species as a function of the number of observations. Each point represents a cell. The purple points represents the cells that did not pass through the second filter (Equation S1).

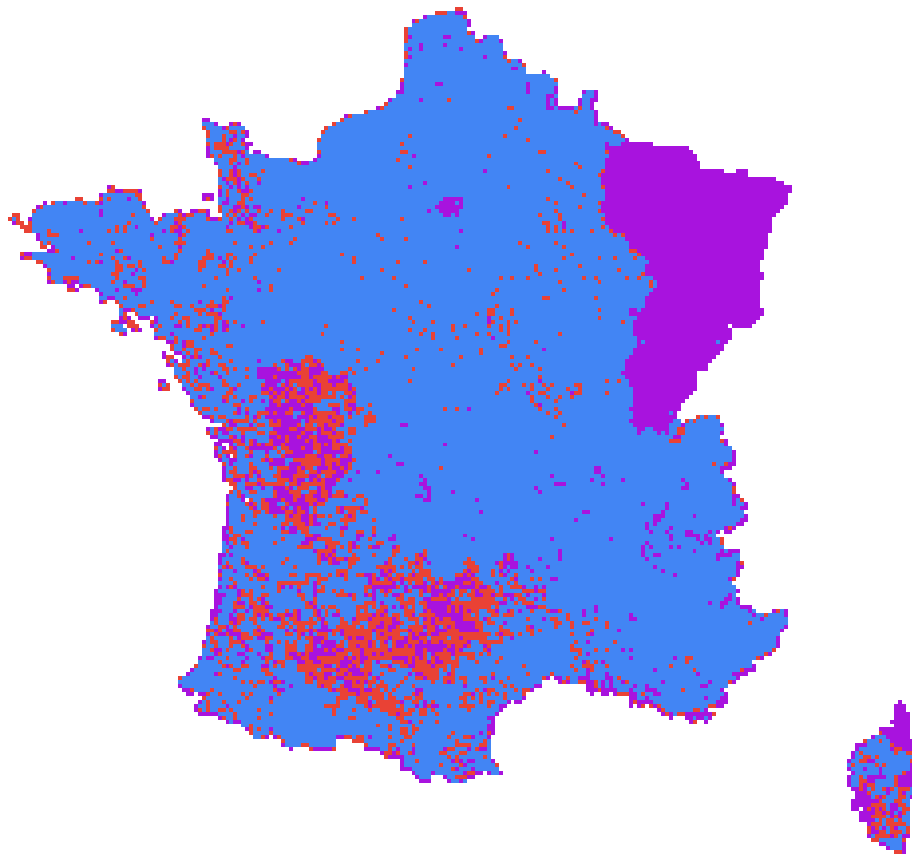


**Figure S4. Map of the cells colored according to the data filtering.** Red if the cell did not pass through the first filter, purple if the cell did not pass through the second filter and blue if the cell passed through both filters.

### Bipartite network construction

To quantify the intensity of spatial interactions between plant and spectral species, we built a bipartite network where a plant species  $p$  is connected to a spectral species  $s$  if they are both present in at least one cell. The edge weight  $W_{ps}$  represents the weighted spatial overlap between the spatial distributions of the plant species  $p$  and the spectral species  $s$ . The weighted overlap coefficient used in this study (Equation 2) is based on the turnover component of the Bray-Curtis similarity index [27].

$$W_{ps} = \frac{A_{ps}}{A_{ps} + \min(T_p - A_{ps}, T_s - A_{ps})} \quad (2)$$

where  $A_{ps}$  is the number of observations in common between species  $p$  and  $s$  in grid cells where both species are present.  $T_p$  and  $T_s$  represent the total number of observations of species  $p$  and  $s$  in the study area, respectively. In order to remove non-significant and null values we only consider weighted overlap coefficients higher than a threshold equal to 0.2.

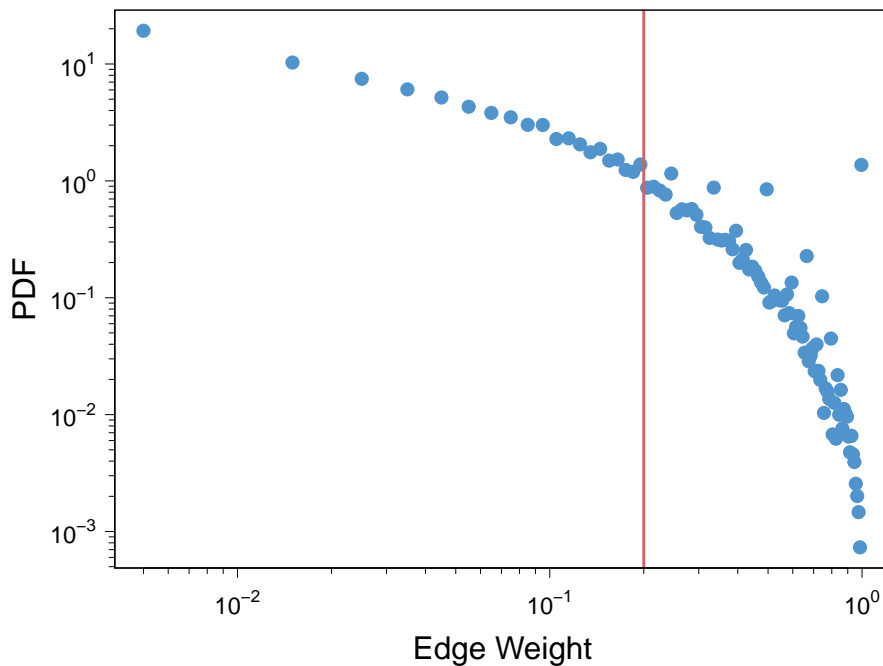
We give here more details on the weighted overlap coefficient computation. Let  $X_{pk}$  and  $X_{sk}$  be the number of observations of species  $p$  and  $s$  in cell  $k$  (ranging between 1 and  $N = 23,060$ ).  $A_{ps}$ ,  $T_p$  and  $T_s$  are given by the following equations,

$$A_{ps} = \sum_{k=1}^N \min(X_{pk}, X_{sk}) \quad (3)$$

$$T_p = \sum_{k=1}^N X_{pk} \quad (4)$$

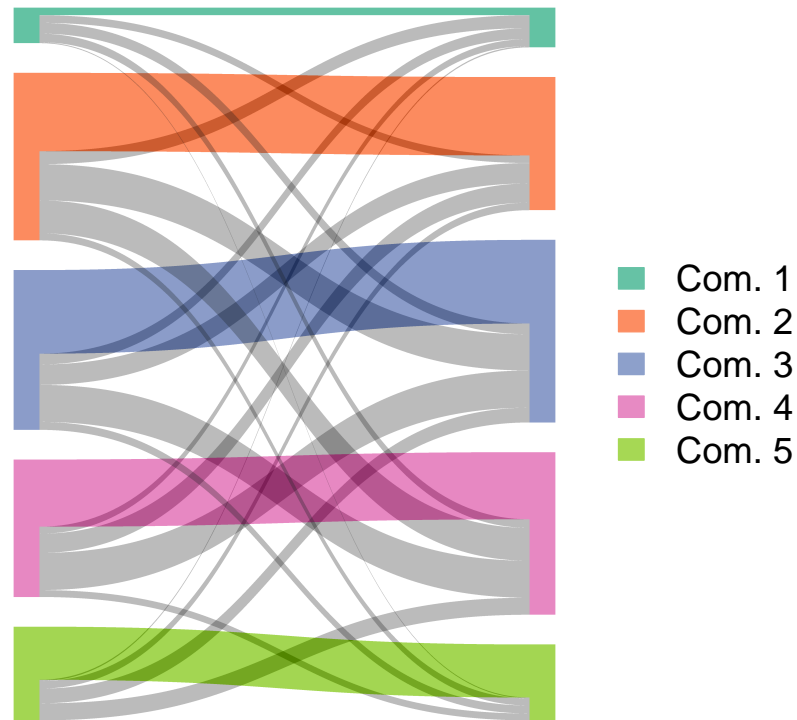
$$T_s = \sum_{k=1}^N X_{sk} \quad (5)$$

Figure S5 shows the probability density function of the bipartite network's edge weights.



**Figure S5. Probability density function of the bipartite network's edge weights.** The red line represents the threshold 0.2 used to prune the network.

### Identification of bioregions



**Figure S6. Network community detection.** Sankey diagram summarizing the distribution of spatial interactions between plant and spectral species. Each color represents a network community and the width of the line is proportional to the sum of weighted overlap coefficient  $W_{ps}$  between plant (left) and spectral (right) species belonging to the same or different network communities.

**Table S1. Number (and percentage) of plant species, spectral species and grid cells by network community.**

Community	Plant	Spectral	Spatial
-	303 (4.56%)	0 (0%)	183 (0.79%)
1	285 (4.29%)	19 (7.6%)	3409 (14.78%)
2	2370 (35.64%)	38 (15.2%)	2718 (11.79%)
3	705 (10.6%)	102 (40.8%)	9388 (40.71%)
4	1318 (19.82%)	62 (24.8%)	5458 (23.67%)
5	1669 (25.1%)	29 (11.6%)	1904 (8.26%)

## Supplementary Tables

**Table S2. Average turnover component of the Bray-Curtis dissimilarity index per pair of cells between bioregion (and its associated standard deviations) obtained with plant and spectral species.**

Relationship	$\beta_{BC-bal}$ (Plant)	$\beta_{BC-bal}$ (Spectral)
BR1 ↔ BR2	0.76 (± 0.18)	0.9 (± 0.09)
BR1 ↔ BR3	0.57 (± 0.21)	0.92 (± 0.08)
BR1 ↔ BR4	0.65 (± 0.22)	0.93 (± 0.07)
BR1 ↔ BR5	0.8 (± 0.15)	0.99 (± 0.03)
BR2 ↔ BR3	0.77 (± 0.16)	0.95 (± 0.07)
BR2 ↔ BR4	0.8 (± 0.16)	0.94 (± 0.07)
BR2 ↔ BR5	0.87 (± 0.12)	0.98 (± 0.05)
BR3 ↔ BR4	0.63 (± 0.2)	0.91 (± 0.09)
BR3 ↔ BR5	0.75 (± 0.17)	0.97 (± 0.05)
BR4 ↔ BR5	0.76 (± 0.17)	0.96 (± 0.07)